Towards many-dimensional real-time quantum theory for heavy-particle dynamics. II. Beyond semiclassics by quantum smoothing of the singularity in quantum-classical correspondence

Kazuo Takatsuka and Satoshi Takahashi
Department of Basic Sciences, Graduate School of Arts and Sciences, The University of Tokyo, Komaba, 153-8902, Tokyo, Japan
(Received 9 June 2013; published 14 January 2014)

A theory of many-dimensional real-time quantum dynamics is studied in terms of action decomposed function (ADF), a class of quantum wave function. In the preceding companion paper [S. Takahashi and K. Takatsuka, Phys. Rev. A **89**, 012108 (2014)], we showed that semiclassical dynamics for ADF in the Lagrange picture of phase flow can be described in terms of what we call deviation determinant and associated quantum phases without use of the stability matrix. Consequently, the Hessian of the involved potential functions is not required in this formalism. This paper is devoted to an analysis of the mechanism of quantum diffusion (quantum smoothing) that removes the singularity inherent in the semiclassical ADF: We derive a Lorentzian form for the amplitude factor of ADF. The real part of its denominator comes from the deviation determinant, while the imaginary part reflects quantum diffusion and is proportional to the Planck constant. The presence of the nonzero imaginary part smooths out the singularity and removes the divergence. Besides, this imaginary part can be obtained through a Wronskian relation with the deviation vectors, which can be solved rather easily at each space-time point on a classical trajectory. A number of theoretical advantages of the Lorentzian form and the Wronskian relation are illustrated theoretically and numerically. It turns out that there is no essential difficulty in applications to many-dimensional heavy-particle systems such as molecules. The theory is examined with stringent numerical tests.

DOI: 10.1103/PhysRevA.89.012109 PACS number(s): 03.65.Ca, 03.65.Sq, 34.10.+x, 31.15.−p

I. INTRODUCTION

This work is devoted to a study of many-dimensional quantum mechanical theory for heavy-particle dynamics as in chemical reactions in terms of the so-called action decomposed function (ADF). In paper I [1], we developed a many-body semiclassical theory, which does not resort to the so-called stability matrix. The semiclassical ADF thus formulated suggests its potential ability to treat large-scale molecular systems. However, as in the lowest-order WKB theory, ADF diverges at caustics or turning points, depending on an initial condition chosen, which reflects the mathematical (geometrical) relationship between quantum and classical mechanics. In this paper, we study a mechanism for genuine quantum effects to smooth the singularity, and propose a methodology that takes a systematic account of such quantum effects, thereby constructing singularity-free wave functions in many-dimensional systems.

To formulate the issue in a self-contained manner, we briefly summarize the previous construction of ADF theory up to the semiclassical stage. We begin with the following time- (t-) dependent wave function:

$$\Psi(\mathbf{q},t) = F(\mathbf{q},t)\exp\left(\frac{i}{\hbar}S(\mathbf{q},t)\right) \tag{1}$$

on a coordinate $\mathbf{q}$ in configuration space, where S is assumed to satisfy the Hamilton-Jacobi (HJ) equation [2]. Then, the Schrödinger equation for $\Psi(\mathbf{q},t)$ is transformed to the equation of motion for the complex-valued amplitude function as

$$\frac{\partial F(\mathbf{q},t)}{\partial t} = \left(-\mathbf{p}\cdot\nabla - \frac{1}{2}(\nabla\cdot\mathbf{p})\right)F(\mathbf{q},t) + \frac{i\hbar}{2}\nabla^2 F(\mathbf{q},t), \tag{2}$$

where $\mathbf{p}$ is a conjugate momentum at $(\mathbf{q},t)$ or $\mathbf{q}(t)$ as

$$\mathbf{p} = \nabla S(\mathbf{q},t). \tag{3}$$

Throughout this paper, we use the mass-weighted coordinates that scale all the masses (m) to unity $m = 1$, and therefore any momentum $\mathbf{p}$ is numerically equivalent to the corresponding velocity $\mathbf{v}$.

Equation (2) is further transformed from the Euler picture in the terminology of fluid mechanics to the Lagrange picture by defining

$$\frac{D}{Dt} = \frac{\partial}{\partial t} + \mathbf{v}\cdot\nabla \tag{4}$$

as

$$\frac{D}{Dt}F(\mathbf{q},t) = \left[-\frac{1}{2}(\nabla\cdot\mathbf{p}) + \frac{i\hbar}{2}\nabla^2\right]F(\mathbf{q},t). \tag{5}$$

In this representation, we write the amplitude of ADF as $F(\mathbf{q}-\mathbf{q}(t),t)$, which is carried along a classical path $\mathbf{q}(t)$. The Trotter decomposition for a short time gives

$$F(\mathbf{q}-\mathbf{q}(t+\Delta t),t+\Delta t) \simeq \exp\left[\frac{i\hbar}{2}\Delta t\nabla^2\right]\exp\left[-\frac{1}{2}(\nabla\cdot\mathbf{p})\Delta t\right]F(\mathbf{q}-\mathbf{q}(t),t) \tag{6}$$

or

$$F(\mathbf{q}-\mathbf{q}(t+\Delta t),t+\Delta t) \simeq \exp\left[-\frac{1}{2}(\nabla\cdot\mathbf{p})\Delta t\right]\exp\left[\frac{i\hbar}{2}\Delta t\nabla^2\right]F(\mathbf{q}-\mathbf{q}(t),t). \tag{7}$$

The semiclassical level approximation takes account of the momentum gradient $\nabla\cdot\mathbf{p} = \sum_k \partial p_k/\partial q_k$ alone as

$$F(\mathbf{q}-\mathbf{q}(t+\Delta t),t+\Delta t) \simeq \exp\left[-\tfrac{1}{2}(\nabla\cdot\mathbf{p})\Delta t\right]F(\mathbf{q}-\mathbf{q}(t),t). \tag{8}$$

The time evolution of it is approximately given as follows: Let $\mathbf{q}^i(t)$ $(i = 1,\ldots,N)$ be a configuration-space point of an

ith nearby path of a reference trajectory $\mathbf{q}(t)$, along which we are propagating the ADF. Thus, ADF propagated by the momentum gradient alone is given as [1]

$$F(\mathbf{q}-\mathbf{q}(t+\Delta t),t+\Delta t)|_{\mathbf{q}=\mathbf{q}(t+\Delta t)} = \left(\frac{\sigma(t)}{\sigma(t+\Delta t)}\right)^{1/2} F(\mathbf{q}-\mathbf{q}(t),t)\Big|_{\mathbf{q}=\mathbf{q}(t)} \tag{9}$$

or

$$\sigma(t+\Delta t)^{1/2} F(\mathbf{q}-\mathbf{q}(t+\Delta t),t+\Delta t)|_{\mathbf{q}=\mathbf{q}(t+\Delta t)} = \sigma(t)^{1/2} F(\mathbf{q}-\mathbf{q}(t),t)|_{\mathbf{q}=\mathbf{q}(t)}, \tag{10}$$

where the deviation determinant $\sigma(t)$ is expressed as

$$\sigma(t) = \prod_{i=1}^{N} \wedge[\mathbf{q}^i(t)-\mathbf{q}(t)], \tag{11}$$

which is an N-dimensional orientable tiny volume surrounding the point $\mathbf{q}(t)$ in configuration space. This propagation suggests a possible way to many-dimensional theory with neither resorting to the integration of the $2N \times 2N$ stability matrix nor the calculation of the related Hessian matrix of potential functions.

Numerical tests [1] have shown that the value of a full quantum wave function is accurately reproduced by the semiclassical ADF at each space-time point along a classical path. However, this function diverges at points where the momentum gradient happens to diverge since it holds there that $\sigma(t)=0$ in Eq. (10). As is well known, this divergence takes place at a focal point either in configuration or momentum space. Therefore, it is in the process of smoothing the singularity that one of the essential characteristics of quantum mechanics can be identified. In this paper, we proceed to the study of many-dimensional quantum dynamics for heavy particles in a stage beyond semiclassical approximation and propose a method to remove the singularity in a tractable manner.

This paper is organized as follows. In Sec. II, we analyze the mathematical mechanism for quantum diffusion to smooth the semiclassical divergence within the ADF formalism. Next in Sec. III, we develop a tractable method to smooth the singularity in the one-dimensional case, which brings about finite valuedness to ADF in a Lorentzian form. The validity of the basic idea up to this step is numerically examined. Then, we proceed to a practice to treat many-dimensional systems, which needs further ideas. Identifying first an important feature of geometry behind the singularity in Sec. IV, we propose a practical method to remove the singularity, which is shown to work quite well. It is numerically demonstrated that the method can be indeed applied to many-dimensional systems. This paper concludes in Sec. V.

II. QUANTUM SMOOTHING OF THE SEMICLASSICAL SINGULARITY WITH THE IMAGINARY DIFFUSION

The main task in this paper is to let the diffusion term $\frac{i\hbar}{2}\nabla^2$ in Eq. (5) work appropriately. There are several ways to do so, depending on a numerical method adopted and/or functional form to represent $F(\mathbf{q}-\mathbf{q}(t),t)$. A direct way is to carry out the numerical calculation of $\nabla^2 F(\mathbf{q}-\mathbf{q}(t),t)$. In fact, Wyatt and his collaborators have developed an efficient way to compute the second-order derivative in the Bohmian dynamics [3–5]. This method should work in our theoretical scheme as well since we let nearby trajectories run around a reference path to calculate $F(\mathbf{q}-\mathbf{q}(t),t)$ in the semiclassical level. However, it is known that the numerical differential is not always a stable procedure, particularly in high-dimensional systems and in short-wavelength regions. Therefore, we take a little more analytical way.

A. Gaussian moving spline function

Let us consider one-dimensional cases for a while until we will specify multidimensional extension. We first represent $F(q-q(t),t)$ of ADF only in a close vicinity of $q=q(t)$ in a moving basis function $G(q-q(t),t)$, which is peaked (localized) at $q=q(t)$. We assume in this close vicinity

$$F(q-q(t),t) \simeq G(q-q(t),t), \tag{12}$$

but at the peak point $q=q(t)$ it is supposed to satisfy

$$F(q-q(t),t)|_{q=q(t)} = G(q-q(t),t)|_{q=q(t)}. \tag{13}$$

Besides, $G(q-q(t),t)$ should behave as a spline function such that

$$|G(q-q(t),t)| \to 0 \text{ as } |q-q(t)| \text{ becomes large.} \tag{14}$$

Let $q_{\text{nearby}}(t)$ be a path running nearby the reference path $q(t)$ at t, and define $\sigma(t) \equiv q_{\text{nearby}}(t)-q(t)$ and $\sigma(t+\Delta t) \equiv q_{\text{nearby}}(t+\Delta t)-q(t+\Delta t)$. Then, Eq. (12) imposes a condition on $G(q-q(t),t)$ similar to Eq. (10) as

$$[q_{\text{nearby}}(t+\Delta t)-q(t+\Delta t)]^{1/2} \times G(q-q(t+\Delta t),t+\Delta t)|_{q=q(t+\Delta t)} \simeq [q_{\text{nearby}}(t)-q(t)]^{1/2} G(q-q(t),t)|_{q=q(t)}. \tag{15}$$

Thus, the height of the G function is modulated only by the distance $q_{\text{nearby}}(t)-q(t)$. On the other hand, if viewed from a point running on a nearby orbit $q_{\text{nearby}}(t)$, the reference path $q(t)$ is regarded as a neighboring path of $q_{\text{nearby}}(t)$. Therefore, the same discussion can be applied to the nearby path with respect to the reference path. Thus, we may expect

$$[q(t+\Delta t)-q_{\text{nearby}}(t+\Delta t)]^{1/2} G(q_{\text{nearby}}(t+\Delta t) - q(t+\Delta t),t+\Delta t) \simeq [q(t)-q_{\text{nearby}}(t)]^{1/2} G(q_{\text{nearby}}(t)-q(t),t). \tag{16}$$

Those G functions that satisfy these conditions can be constructed as follows: Consider a time-dependent Gaussian function of the form

$$G(q-q(t),t) = \left(\frac{2}{\pi}\right)^{1/4} g(q(t)) \exp\{-(\gamma(t))[q-q(t)]^2\}, \tag{17}$$

for which the exponent should satisfy

$$\gamma(t+\Delta t) = \gamma(t)\left(\frac{\sigma(t)}{\sigma(t+\Delta t)}\right)^2 \tag{18}$$

and the amplitude is to be propagated as

$$g(q(t+\Delta t)) = g(q(t))\left(\frac{\sigma(t)}{\sigma(t+\Delta t)}\right)^{1/2}. \tag{19}$$

It is not difficult to see $G(q-q(t),t)$ fulfill the above three conditions. This Gaussian is valid as a local approximation to $F(q-q(t),t)$ only in the corresponding local area, and its norm is conserved in the sense that

$$\int dq|G(q-q(t+\Delta t),t+\Delta t)|^2 = \int dq|G(q-q(t),t)|^2. \tag{20}$$

Note that both $\gamma(t)$ and $g(q(t))$ may be complex valued.

B. Quantum diffusion

Operation of the integral kernel of free-particle propagation $\exp[\frac{i\hbar}{2}\Delta t\nabla^2]$ onto a Gaussian function, that is,

$$\exp\left[\frac{i\hbar}{2}\Delta t\nabla^2\right]f(q) = \left(\frac{m}{2\pi i\hbar\Delta t}\right)^{1/2}\int_{-\infty}^{\infty}dy \times \exp\left[\frac{im(q-y)^2}{2\hbar\Delta t}\right]f(y) \tag{21}$$

can be treated analytically, an important consequence being that a Gaussian remains Gaussian. We next consider this propagation of the quantum diffusion to the function of Eq. (17). To do so, we beforehand apply the momentum gradient term $\exp[-\frac{1}{2}(\nabla p)\Delta t]$ as

$$\begin{aligned} &G^{mg}(q-q(t+\Delta t),t+\Delta t) \\ &= \exp\left[-\frac{1}{2}(\nabla p)\Delta t\right]G(q-q(t),t) \\ &= \left(\frac{2}{\pi}\right)^{1/4}g(q(t))\left(\frac{\sigma(t)}{\sigma(t+\Delta t)}\right)^{1/2} \\ &\quad\times\exp\{-[\gamma^{mg}(t+\Delta t)][q-q(t+\Delta t)]^2\}, \end{aligned} \tag{22}$$

where

$$\gamma^{mg} = \gamma(t)\left(\frac{\sigma(t)}{\sigma(t+\Delta t)}\right)^2 \tag{23}$$

as we saw above in Eqs. (18) and (19). Then, the quantum diffusion gives rise to

$$\begin{aligned} &G(q-q(t+\Delta t),t+\Delta t) \\ &= \exp\left[\frac{i\hbar}{2}\Delta t\nabla^2\right]G^{mg}(y-q(t+\Delta t),t+\Delta t) \\ &= \left(\frac{2}{\pi}\right)^{1/4}g(q(t))\left(\frac{\sigma(t)}{\sigma(t+\Delta t)}\frac{1/\gamma^{mg}}{1/\gamma^{mg}+i2\hbar\Delta t/m}\right)^{1/2} \\ &\quad\times\exp\left[-\frac{1}{1/\gamma^{mg}+i2\hbar\Delta t/m}[q-q(t+\Delta t)]^2\right], \end{aligned} \tag{24}$$

which gives

$$\frac{1}{\gamma(t+\Delta t)} = \frac{1}{\gamma^{mg}} + i\frac{2\hbar\Delta t}{m} \tag{25}$$

and

$$g(q(t+\Delta t)) = g(q(t))\left(\frac{\sigma(t)}{\sigma(t+\Delta t)}\frac{1/\gamma^{mg}}{1/\gamma^{mg}+i2\hbar\Delta t/m}\right)^{1/2}. \tag{26}$$

C. Inverse complex exponents and dynamics

The above analysis, particularly Eq. (24), suggests that $G(q-q(t),t)$ can be more conveniently expressed as

$$\begin{aligned} &G(q-q(t),t) \\ &= \left(\frac{2}{\pi}\right)^{1/4}g(q(t))\exp\left[-\frac{1}{c(t)+id(t)}[q-q(t)]^2\right], \end{aligned} \tag{27}$$

with both $c(t)$ and $d(t)$ being real valued. Equation (23) gives a recursion relation for $c(t)$

$$c(t+\Delta t) = c(t)\left(\frac{\sigma(t+\Delta t)}{\sigma(t)}\right)^2 \tag{28}$$

and Eq. (25) gives rise to

$$d(t+\Delta t) = d(t)\left(\frac{\sigma(t+\Delta t)}{\sigma(t)}\right)^2 + \frac{2\hbar\Delta t}{m}. \tag{29}$$

As seen in these expressions, their roles are summarized as follows: (1) $c(t)$, the real part of $1/\gamma(t)$, is responsible only for the WKB (semiclassical) flow. (2) $d(t)$, the imaginary part of $1/\gamma(t)$, is responsible for quantum diffusion and also its coupling with the WKB flow. Note that the Planck constant appears only in $d(t)$.

The difference equation for $d(t)$ in Eq. (29) becomes difficult to treat numerically near points of $\sigma(t)=0$, which are the singular points in the semiclassical ADF. Besides, other types of difference equations such as Eq. (29) can result depending on the operator ordering when Eq. (5) is represented in the Trotter decomposition. For instance, while the operator ordering of Eq. (6) gave (29), Eq. (7) gives

$$d(t+\Delta t) = \left(d(t)+\frac{2\hbar\Delta t}{m}\right)\frac{\sigma(t+\Delta t)^2}{\sigma(t)^2}. \tag{30}$$

However, such dependence on the operator ordering can be eliminated by reducing the difference equations into differential equations taking a limit of $\Delta t\to 0$. For $d(t)$, we have

$$\dot{d}(t) = 2\frac{\dot{\sigma}(t)}{\sigma(t)}d(t) + \frac{2\hbar}{m}, \tag{31}$$

where the dot above the symbols indicates the first-order time derivative. Obviously, for $c(t)$ we have

$$\dot{c}(t) = 2\frac{\dot{\sigma}(t)}{\sigma(t)}c(t). \tag{32}$$

We next analyze the singularity with these differential equations.

D. Analysis on the removal of singularity by quantum diffusion

As shown in Eq. (20), $G(q-q(t),t)$ in the level of momentum gradient conserves the norm up to the phase. It is obvious that the kernel operation in Eq. (21) also conserves the norm of a wave function applied. Therefore, $G(q-q(t),t)$ should conserve the norm in the time propagation. We may hence set that $G(q-q(t),t)$ is normalized to unity without

loss of generality. Then, it can be written as

$$G(q-q(t),t) = \left(\frac{2}{\pi}\right)^{1/4} [c(t)]^{1/4}[c(t)+id(t)]^{-1/2} \times \exp\left[-\frac{1}{c(t)+id(t)}[q-q(t)]^2\right], \quad (33)$$

in which the height should be chosen to fulfill the condition (13), that is,

$$\left(\frac{2}{\pi}\right)^{-1/4} F(q-q(t),t)|_{q=q(t)} = [c(t)]^{1/4}[c(t)+id(t)]^{-1/2} \equiv X(t). \quad (34)$$

In Eq. (33), $G(q-q(t),t)|_{q=q(t)}$ and $F(q-q(t),t)|_{q=q(t)}$ as well seem to have a divergence in their amplitudes $X(t)$, when both $c(t)$ and $d(t)$ happen to be zero. Hence, it is crucial to confirm that such a divergence is smoothed away and does not actually appear. Let us concentrate a time t^*, at which $\sigma(t^*)=0$. Then, the differential equation for $c(t)$ gives

$$c(t) = \frac{c(0)}{\sigma(0)^2}\sigma(t)^2 \quad (35)$$

and hence $c(t^*)=0$ naturally follows. On the other hand, the differential equation for $d(t)$ [Eq. (31)] may be transformed by setting

$$d(t) = \sigma(t)^2 f(t)$$

to

$$\dot{f}(t) = \frac{2\hbar}{\sigma(t)^2} \quad (36)$$

($m=1$ as usual.) Let us expand $\sigma(t)$ around the singular time as

$$\sigma(t^*+\varepsilon) = \sigma_1\varepsilon + \sigma_2\varepsilon^2 + \sigma_3\varepsilon^3 + \cdots \quad (37)$$

for a small time increment ε. Then, a simple analysis gives

$$f(t^*+\varepsilon) = -\frac{a}{\sigma_1^2}\frac{1}{\varepsilon} - 2a\frac{\sigma_2}{\sigma_1^3}\ln\varepsilon - 2a\frac{\sigma_3}{\sigma_1^3}\varepsilon - \cdots + \text{const}, \quad (38)$$

with $a = 2\hbar/m$, giving rise to

$$d(t^*+\varepsilon) \simeq -2\hbar\varepsilon. \quad (39)$$

Therefore, it is in fact expected that $c(t)$ and $d(t)$ approach simultaneously zero as $\sigma(t)$ becomes zero ($|\varepsilon|\to 0$), and the singularity seems to remain. However, from Eq. (35) we observe

$$c(t^*+\varepsilon) \simeq \frac{c(0)}{\sigma(0)^2}\sigma_1(t^*)^2\varepsilon^2, \quad (40)$$

and, due to the difference in the rates of approaching zero for $c(t^*+\varepsilon)$ [Eq. (40)] and $d(t^*+\varepsilon)$ [Eq. (39)], the zero in the denominator of $X(t)$ is actually canceled [to be shown explicitly in Eq. (45)]. This is the mechanism of a manner how the semiclassical divergence due to $c(t^*)=0$ is mathematically suppressed by $d(t^*)=0$.

To be a little more precise, we write how the amplitude part of $F(q-q(t),t)$ behaves near $t=t^*$. Representing the denominator in the polar representation as

$$c(t)+id(t) = re^{i\theta}, \quad (41)$$

we rewrite $X(t)$ as

$$X(t) = \left(\frac{c(t)}{c(t)^2+d(t)^2}\right)^{1/4} \exp\left(-i\frac{\theta(t)}{2}\right). \quad (42)$$

Then, we study the dynamics nearby a singular point at time $t=t^*+\varepsilon$. Then, it holds that

$$\tan\theta(t^*+\varepsilon) = \frac{d(t^*+\varepsilon)}{c(t^*+\varepsilon)} \simeq \frac{-2\hbar\varepsilon}{\frac{c(0)}{\sigma(0)^2}\sigma_1(t^*)^2\varepsilon^2} \to \begin{cases} \infty & \text{for} \quad \varepsilon<0, \\ -\infty & \text{for} \quad \varepsilon>0. \end{cases} \quad (43)$$

This implies that the angle passes across $\pi/2$ smoothly through the singular point with the phase

$$\theta(t^*) \to \frac{\pi}{2} + n\pi, \quad (44)$$

where $\tan\theta = d(t)/c(t)$. Thus, we have

$$X(t^*) \to \left[\frac{\frac{c(0)}{\sigma(0)^2}\sigma_1(t^*)^2}{4\hbar^2}\right]^{1/4} \exp\left(-i\frac{\pi}{4}\right) = \left[\frac{\frac{c(0)}{\sigma(0)^2}}{4\hbar^2}\right]^{1/4} \exp\left(-i\frac{\pi}{4}+i\frac{n\pi}{2}\right)\sigma_1(t^*)^{1/2}, \quad (45)$$

where the phase proceeds continuously and monotonically, and n in this expression represents the number for a trajectory to pass across the zeros of $\sigma(t)$.

III. LORENTZIAN FORM FOR ADF AMPLITUDE

We proceed further to find a tractable method to remove the singularity. Again, we first consider a one-dimensional case. Extension to multidimensional cases will be made in the next section.

A. Lorentzian form of the amplitude

Along a reference path $q(t)$, we study $X(t)$ of Eq. (34), which is rewritten in the form

$$X(t) = \left(\frac{1}{c(t)^{1/2}+id(t)/c(t)^{1/2}}\right)^{1/2}. \quad (46)$$

Recalling $\sigma(t) = q_{\text{nearby}}(t) - q(t)$ and the relation of Eq. (35), Eq. (46) is further rewritten as

$$X(t) = \frac{1}{A_0^{1/2}}\left(\frac{1}{\sigma(t)+i\eta(t)}\right)^{1/2}, \quad (47)$$

where

$$\eta(t) = A_0\frac{d(t)}{c(t)^{1/2}} = B_0\frac{d(t)}{\sigma(t)} \quad (48)$$

with

$$A_0 = \frac{c(0)^{1/2}}{\sigma(0)} \quad \text{and} \quad B_0 = \frac{\sigma(0)^2}{c(0)}. \quad (49)$$

$\eta(t)$ is obviously responsible for the removal of singularity at a time of $q(t) = q_{\rm nearby}(t)$ [or $\sigma(t) = 0$]. Our goal is thus to determine $\eta(t)$.

After the manner of Eq. (10), we write the conservation rule for the quantum ADF as

$$[\sigma(t+\Delta t) + i\eta(t+\Delta t)]^{1/2} F(q - q(t+\Delta t), t + \Delta t)|_{q=q(t+\Delta t)} = [\sigma(t) + i\eta(t)]^{1/2} F(q - q(t), t)|_{q=q(t)}. \tag{50}$$

The amplitude of ADF is thus modulated not only by $\sigma(t)$, which represents the path density surrounding a reference path, but also $\eta(t)$, through which quantum kinematic diffusion couples with $\sigma(t)$ dynamics. Even if the nearby dynamics $\sigma(t)$ is constant in time or happens to be zero, $\eta(t)$ keeps affecting the absolute height of the quantum wave function as shown in Eq. (59). Also, since $\sigma(t)$ in one dimension is just a distance in real-valued configuration space between the reference path and a nearby one, $i\eta(t)$ may have an analogous interpretation as imaginary distance or imaginary deviation. $[\sigma(t) + i\eta(t)]^{1/2}$ serves as a square root of the measure for integration associated with the classical path $[q(t), p(t)]$. We will discuss this aspect elsewhere.

Since $\eta(t)$ is proportional to the Planck constant, through $d(t)$ in Eqs. (48) and (31), the $\hbar$ dependence of the amplitude is now revealed to be

$$X(t) \sim \left(\frac{1}{\sigma(t) + iC(t)\hbar}\right)^{1/2}, \tag{51}$$

where both $\sigma(t)$ and $C(t)$ can be always chosen to be free of $\hbar$. Note also that we have not used a perturbation expansion of the wave function with respect to $\hbar$. Thus, this dependence on $\hbar$ must be generic. Equation (51) should be compared with the semiclassical kernel (in one dimension), for example, the amplitude of which is totally different as seen in [6–9]

$$K(q_f, q_i, t) \equiv \langle q_f | \exp\left[-\frac{i}{\hbar}\hat{H}t\right] |q_i\rangle \simeq (2\pi\hbar)^{-1/2} \left|\frac{\partial q_f}{\partial p_i}\right|^{-\frac{1}{2}} \exp\left[\frac{i}{\hbar} S(q_f, q_i, t) - \frac{i\pi\lambda}{2}\right], \tag{52}$$

where λ is the Maslov index in this representation. It is anticipated that the amplitude of the form of Eq. (51) may have a significant contribution to energy quantization in a large limit of $\hbar$. Indeed, it is known that phase quantization alone does not reproduce the quantum eigenvalues in a large-$\hbar$ limit [10,11]. On the other hand, it is obvious that the factor $(2\pi\hbar)^{-1/2}$ in Eq. (52) can modulate the spectral height but should have no effect on the spectral positions. Therefore, the $\hbar$ dependence of the amplitude factor in Eq. (52) is not theoretically sufficient. Application of the quantum ADF having Eq. (51) to energy quantization is under way.

B. A Wronskian relation for $\sigma(t)$ and $\eta(t)$

To determine $\eta(t)$, let us define a function

$$\varsigma(t) \equiv \frac{d(t)}{\sigma(t)} = \frac{\eta(t)}{B_0}. \tag{53}$$

Using Eqs. (31) and (32), we have

$$\frac{d}{dt}\varsigma(t) = \frac{\dot{\sigma}(t)}{\sigma(t)}\varsigma(t) + \frac{a}{\sigma(t)} \tag{54}$$

($a = 2\hbar/m$), which is rearranged to a Wronskian relation

$$\sigma(t)\dot{\varsigma}(t) - \dot{\sigma}(t)\varsigma(t) = a. \tag{55}$$

This is what we really need to solve.

The most important role of $\eta(t)$ should be played when $\sigma(t) = 0$. Therefore, let us consider the behavior of $\eta(t)$ at a time t^*:

$$\sigma(t^*) = 0. \tag{56}$$

Under this condition we have

$$\varsigma(t^*) = -\frac{a}{\dot{\sigma}(t^*)}, \tag{57}$$

and rendering this value back into Eq. (55), we see

$$\dot{\varsigma}(t^*) = \frac{\dot{\sigma}(t^*)}{\sigma(t^*)}\left(-\frac{a}{\dot{\sigma}(t^*)}\right) + \frac{a}{\sigma(t^*)} = 0. \tag{58}$$

Thus, it turns out that the absolute value of $\varsigma(t)$ [and $\eta(t)$] becomes extremum at the zeros of $\sigma(t)$.

Another special case, which serves as a test system to examine the validity of the Wronskian relation, is a system of no potential and the deviation vector lies on the trajectory, with $\dot{\sigma}(t) = 0$ always. Then, we see

$$\frac{\eta(t)}{B_0} = \varsigma(t) = \frac{a}{\sigma(0)_{\rm constant}} t + \text{const.} \tag{59}$$

This result reproduces the free-particle Gaussian wave packet exactly.

A straightforward approximation to solve the Wronskian relation is shortly described in Appendix A.

C. Rescaling procedure of nearby trajectories

As shown in paper I [1], the nearby orbit can be repositioned in phase space in a way to conserve the value of the momentum gradient for a reference path $[q(t), p(t)]$:

$$\frac{\partial p}{\partial q} \simeq \frac{p_{\rm nearby}(t) - p(t)}{q_{\rm nearby}(t) - q(t)} = \frac{[p_{\rm nearby}(t) - p(t)] \times A}{[q_{\rm nearby}(t) - q(t)] \times A}, \tag{60}$$

which renews $[q_{\rm nearby}(t), p_{\rm nearby}(t)]$ to

$$q^{\rm new}_{\rm nearby}(t) = q(t) + [q_{\rm nearby}(t) - q(t)] \times A \tag{61}$$

and

$$p^{\rm new}_{\rm nearby}(t) = p(t) + [p_{\rm nearby}(t) - p(t)] \times A. \tag{62}$$

The Wronskian relation should be accordingly modified as

$$\sigma_{\rm new}(t) + i\eta_{\rm new}(t) = [\sigma_{\rm old}(t) + i\eta_{\rm old}(t)]A, \tag{63}$$

where the left-hand side includes the rescaled quantities. Thus, we can improve the values of $[\sigma(t), \eta(t)]$ when nearby paths deviate farther from the reference path. This rescaling procedure will be actually applied and verified in Sec. III D.

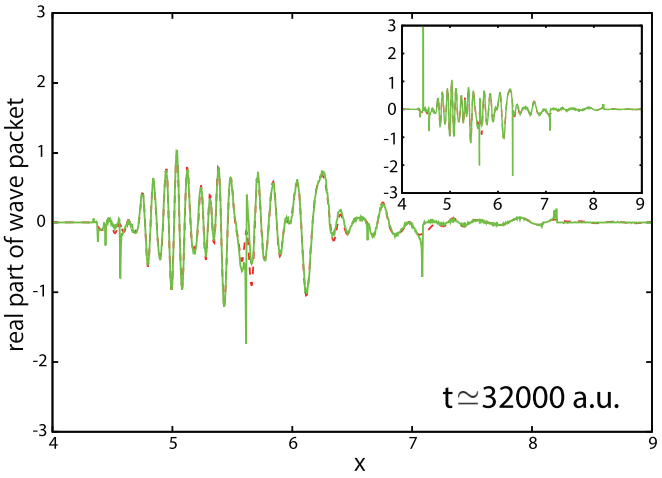

FIG. 1. (Color) Snapshot of the real part of FQ (red curve) and ADF (green curve) wave packets after about 3.5 oscillations as a function of the coordinate x (in atomic units). In the inset, the corresponding semiclassical ADF (green curve) is compared with the FQ (full quantum) result (red curve), which are both taken from paper I. It is confirmed from both results that some of the strongly divergent parts have been clearly suppressed by incorporating quantum diffusion via the Wronskian relation.

D. Numerical verification of the idea

Before proceeding to multidimensional extension of the above idea, we here verify how practically both the Lorentzian and Wronskian work in a one-dimensional system. Wave-packet dynamics on the following Morse potential is examined:

$$V(q) = D_e[1 - e^{-\alpha(q-q_e)}]^2, \tag{64}$$

where $m = 1.165 \times 10^5$, $D_e = 0.05717$, $q_e = 5.039$, and $\alpha = 0.9830$ in atomic units [12,13]. The same system with the same initial conditions as that in paper I [1] is adopted here, which was used to test the semiclassical ADF. It has been already confirmed that full quantum wave packets are very well reproduced by the semiclassical ADF that takes account of only momentum gradient, except in spatial regions near singular points (caustics) [1].

In Fig. 1 are presented snapshots of propagated wave packets with the two methods after about 3.5 oscillations: one in the red curve has been obtained with full quantum (FQ) calculation in terms of the symplectic integrator fast Fourier transform (FFT) method [14], while the wave packet given by the present ADF (termed as quantum ADF) is represented in the green curve. The initial wave function is given as a coherent-state wave packet of $p_0 = 0$, $q_0 = 4.535$, $E_0 = 0.02342$ (in a.u.), and $\hbar = 1.0$. The values of the ADF are calculated at equally spaced grid points at $t = 0$, which are propagated along classical trajectories starting from individual initial coordinates and the same $p_0 = 0$. At any time step, the global ADF wave function is reconstructed by summing up $X(t)$ of the trajectories found within each bin. The number of trajectories used is 10 000, each of which is accompanied with a nearby trajectory running close to it. Rescaling of the nearby path is performed when $\sigma(t)$ becomes larger than a predetermined threshold value ζ [set to $\zeta = 2.0 \times \sigma(0)$ here]. In the inset of Fig. 1, the semiclassical ADF of paper I is reproduced, in which two points of divergence are apparent. On the other hand, the ADF treated as above with the quantum diffusion demonstrates that agreement of the real part of wave packets is excellent, although there remain a few spatial regions where the smoothing is not enough. It is confirmed, however, that the divergence has been certainly suppressed by incorporating quantum diffusion via the Wronskian relation, leading to a better description of the wave packet. We therefore may judge that the theory is worth extending to multidimensional systems.

IV. MULTIDIMENSIONAL DYNAMICS

We next consider a multidimensional extension of the above-developed quantum approximation. We first formulate a formal theory and then investigate geometrically and numerically to see how the formal theory can be approximated in actual calculations.

A. Formal theory

Let $[\mathbf{q}^0(t),\mathbf{p}^0(t)]$ be a path along which the momentum gradient and quantum diffusion are to be considered. To represent the deviation determinant explicitly, we assume appropriate nearby paths $[\mathbf{Q}^I(t),\mathbf{P}^I(t)]$ $(I = 1,\ldots,N)$, running on a prespecified action plane S with appropriate initial conditions. Their deviation vectors are denoted as

$$\Delta\mathbf{Q}^I(t) = \mathbf{Q}^I(t) - \mathbf{q}^0(t). \tag{65}$$

For each of them, let $\mathbf{e}^I$ be a unit vector parallel to $\Delta\mathbf{Q}^I$ such that

$$\Delta\mathbf{Q}^I = \Delta Q^I \mathbf{e}^I, \tag{66}$$

and these are assumed to be orthogonal

$$\mathbf{e}^I \cdot \mathbf{e}^J = \delta_{IJ}. \tag{67}$$

It is further assumed that these coordinates satisfy

$$\frac{\partial^2 S}{\partial Q_I \partial Q_J} = \frac{\partial P_I}{\partial Q_J} = \frac{\partial P_J}{\partial Q_J}\delta_{IJ}, \tag{68}$$

which indicates the action function S is locally separable with respect to this coordinate system and the higher-order terms such as

$$\frac{\partial}{\partial Q_I}\left(\frac{\partial P_I}{\partial Q_J}\right) \tag{69}$$

must be very small.

Then, Eq. (5) is written as

$$\begin{aligned} &F(\mathbf{Q} - \mathbf{Q}(t+\Delta t), t+\Delta t) \\ &\simeq \exp\left[\int_t^{t+\Delta t} dt \sum_J \left(-\frac{1}{2}\frac{\partial P_J}{\partial Q_J} + \frac{i\hbar}{2}\frac{\partial^2}{\partial Q_J^2}\right)\right] \\ &\quad \times F(\mathbf{Q} - \mathbf{Q}(t), t) \end{aligned} \tag{70}$$

for a short period Δt, and due to the property of Eq. (68) one may approximately factor Eq. (70) to a product form

$$\begin{aligned} &F(\mathbf{Q} - \mathbf{Q}(t+\Delta t), t+\Delta t) \\ &\simeq \prod_J \exp\left[\int_t^{t+\Delta t} dt \left(-\frac{1}{2}\frac{\partial P_J}{\partial Q_J} + \frac{i\hbar}{2}\frac{\partial^2}{\partial Q_J^2}\right)\right] \\ &\quad \times F(\mathbf{Q} - \mathbf{Q}(t), t). \end{aligned} \tag{71}$$

As in the one-dimensional case [Eq. (12)], we prepare a Gaussian function to approximate $F(\mathbf{Q}-\mathbf{Q}(t),t)$ only in the close vicinity of $\mathbf{Q}=\mathbf{Q}(t)$. Making use of the separable form of Eq. (71) for a short-time interval, we can construct the following Gaussian function:

$$G(\mathbf{Q}-\mathbf{Q}(t),t)=\left(\frac{2}{\pi}\right)^{N/4}\prod_J\frac{c_J(t)^{1/4}}{[c_J(t)+id_J(t)]^{1/2}}\times\exp\left[-\frac{1}{c_J(t)+id_J(t)}[Q_J(t)-Q_J^0(t)]^2\right] \tag{72}$$

as a moving basis. Then, as in the one-dimensional case we have

$$\dot{c}_J(t)=2\frac{\dot{\sigma}_J(t)}{\sigma_J(t)}c_J(t) \tag{73}$$

and

$$\dot{d}_J(t)=2\frac{\dot{\sigma}_J(t)}{\sigma_J(t)}d_J(t)+2\frac{\hbar}{m_J} \tag{74}$$

with $m_J=1$.

In each instantaneous coordinate satisfying Eq. (68) we can apply the theory developed for one-dimensional systems in the preceding section. Then, the height of the ADF function is given as

$$X(t)=\prod_J\frac{c_J(t)^{1/4}}{[c_J(t)+id_J(t)]^{1/2}}=A_0^{-N/2}\prod_J[\sigma_J(t)+i\eta_J(t)]^{-1/2}, \tag{75}$$

where again

$$\eta_J(t)=B_0\frac{d_J(t)}{\sigma_J(t)}=B_0\varsigma_J(t) \tag{76}$$

with $A_0=c_J(0)^{1/2}/\sigma_J(0)$ and $B_0=\sigma_J(0)^2/c_J(0)$. It is convenient to choose the initial conditions so that they give common values of A_0 and B_0.

Note that this divergence-free amplitude factor is given in a short interval of $[t,t+\Delta t]$, and the long-time propagation of $F(\mathbf{Q}-\mathbf{Q}(t),t)$ along the reference path $\mathbf{q}^0(t)$ is obtained by the recursive relation

$$F(\mathbf{Q}-\mathbf{Q}(t+\Delta t),t+\Delta t)|_{\mathbf{Q}=\mathbf{Q}(t+\Delta t)}=\frac{X(t+\Delta t)}{X(t)}F(\mathbf{Q}-\mathbf{Q}(t),t)\Big|_{\mathbf{Q}=\mathbf{Q}(t)}. \tag{77}$$

As in the case of momentum gradient only (see paper I [1]), both $X(t+\Delta t)$ and $X(t)$ are to be determined within the same time interval $[t,t+\Delta t]$. Therefore, it can be written in more general fashion as

$$F(\mathbf{Q}-\mathbf{Q}(t+2\Delta t),t+2\Delta t)|_{\mathbf{Q}=\mathbf{Q}(t+2\Delta t)}=\frac{X^{(2)}(t+2\Delta t)}{X^{(2)}(t+\Delta t)}\frac{X^{(1)}(t+\Delta t)}{X^{(1)}(t)}F(\mathbf{Q}-\mathbf{Q}(t),t)\Big|_{\mathbf{Q}=\mathbf{Q}(t)},$$

in which $X^{(1)}(t+\Delta t)$ and $X^{(1)}(t)$ are determined in $[t,t+\Delta t]$, while $X^{(2)}(t+2\Delta t)$ and $X^{(2)}(t+\Delta t)$ are given in the next interval $[t+\Delta t,t+2\Delta t]$. Therefore, $X^{(1)}(t+\Delta t)$ can be different from $X^{(2)}(t+\Delta t)$. Likewise, we can extend the procedure to a finite time as

$$\mathbf{X}(t+n\Delta t,t)=\frac{X^{(n)}(t+n\Delta t)}{X^{(n)}[t+(n-1)\Delta t]}\cdots\times\frac{X^{(2)}(t+2\Delta t)}{X^{(2)}(t+\Delta t)}\frac{X^{(1)}(t+\Delta t)}{X^{(1)}(t)}, \tag{78}$$

which serves as a kernel along a classical path since $\mathbf{X}$ is independent of the initial amplitude of $F(\mathbf{Q}-\mathbf{Q}(t),t)$. After all, we have

$$F(\mathbf{Q}-\mathbf{Q}(t+n\Delta t),t+n\Delta t)|_{\mathbf{Q}=\mathbf{Q}(t+n\Delta t)}=\mathbf{X}(t+n\Delta t,t)F(\mathbf{Q}-\mathbf{Q}(t),t). \tag{79}$$

In this regard, the dynamics of ADF is akin to the Bohmian rather than to that of the Feynman kernel.

B. Practical approximations

The practical aspects of the above formalism are surveyed with numerical examples in the rest of this paper. The most serious challenge here is how to choose the coordinate systems that give independent deviation vectors $\{\Delta\mathbf{Q}^J|J=1,\ldots,N\}$ satisfying the diagonalization condition of an action function as in Eq. (68). This is not an easy task.

The following modified Hénon-Heiles Hamiltonian

$$H(x,y,p_x,p_y)=\frac{p_x^2}{2m}+\frac{p_y^2}{2m}+\frac{x^2+y^2}{2}+x^2(0.6y^2+y)+\frac{1}{3}y^3(0.2y-1)+0.1x \tag{80}$$

is chosen as the first example with $m=1$. In the present numerical tests, we check if the time evolution of the height of a wave packet is reproduced. In contrast to the case of Fig. 1, we do not intend to generate a global wave packet, but rather the height of an ADF at a space-time point is tracked along a single path. The results are compared with the full quantum counterparts. Such a pointwise comparison imposes a really stringent test. In the corresponding full quantum calculations, a wave packet is propagated with an initial form

$$F(\mathbf{q}-\mathbf{q}(0),0)=\left(\frac{1}{\pi\hbar}\right)^{1/2}\exp\left[-(\mathbf{q}-\mathbf{q}_0)\cdot\mathbf{M}\cdot(\mathbf{q}-\mathbf{q}_0)^T+\frac{i}{\hbar}\mathbf{p}_0\cdot(\mathbf{q}-\mathbf{q}_0)\right], \tag{81}$$

where

$$\mathbf{M}=\begin{pmatrix}\frac{1}{2\hbar\times w} & 0\\ 0 & \frac{1}{2\hbar\times w}\end{pmatrix}, \tag{82}$$

$\mathbf{q}-\mathbf{q}_0=(x-x_0,y-y_0)^T$, and $\mathbf{p}_0=(p_{x_0},p_{y_0})^T$. At each time step, we track the wave-packet height along the corresponding classical trajectory with the energy $E\simeq 0.10$.

Here, in this test we check the performance of ADF in a situation close to the semiclassical limit, and the Planck constant is set to $\hbar=0.001$, while the parameter is set to $w=5$ to let the Gaussian have slightly broad width. It is

generally impossible to attribute the entire dynamics of a wave function to a "single" classical path since it is generally a coherent sum of components coming from many other action surfaces. We should also note that only the absolute values of the wave-packet height are plotted for comparison because such a small-$\hbar$ value causes highly oscillatory behavior in both the real and imaginary parts individually. However, it has been already confirmed that agreement of phase is very good between ADF and FQ, although not shown here.

1. A naive approximation with use of straightforward orthogonalization

We first show the results by a naive application of the Wronskian relation to a test two-dimensional system. To perform theoretically correct treatment of the Wronskian relation, as described above in the preceding section, we need to find nearby paths $[\mathbf{Q}^I(t),\mathbf{P}^I(t)]$ $(I = 1,\ldots,N)$ that satisfy the action-diagonalization condition of Eq. (68) and the orthogonality condition of Eq. (67). However, it is practically difficult to find such nearby paths at each time since we usually prepare only one set of nearby orbits (N trajectories) for a single reference path, whose deviation vectors do not usually satisfy those conditions. Therefore, we first see what will result if we ignore the action-diagonalization condition. That is, we impose only the orthogonality condition on the deviation vectors at each time step, which is carried out with the Gram-Schmidt method. The value of the deviation determinant is kept invariant by this orthogonalization.

Suppose we have obtained such mutually orthogonal deviation vectors $\Delta\mathbf{Q}^J(t)$, their associated momenta $\Delta\mathbf{P}^J(t)$, and the corresponding deviation forces $\Delta\mathbf{F}^J(t)$. Note that these vectors should depend on the choice of the initial vector in the Schmidt orthogonalization procedure, and accordingly so does the resultant value of $X(t)$. To obtain $\eta_J(t)$ for each $\sigma_J(t)$, the information of $\dot\sigma_J(t)$ and $\ddot\sigma_J(t)$ are required (see Appendix A), which should be calculated through $\Delta\mathbf{P}^J(t)$ and $\Delta\mathbf{F}^J(t)$, respectively. However, since $\Delta\mathbf{P}^J(t)$ and $\Delta\mathbf{F}^J(t)$ are not generally parallel to $\Delta\mathbf{Q}^J(t)$, these are projected onto the unit vector of $\mathbf{e}^J$ as defined in Eq. (66). Thus, we have a set of $\{\sigma_J(t),\dot\sigma_J(t),\ddot\sigma_J(t)\}$ in hand to solve the Wronskian relation.

In Fig. 2, we show ADF heights obtained with two different sets of initial orientations of the deviation vectors but both having a same $\sigma(0)$. Initial orientations are randomly chosen by rotations relative to the x and y axes. It is seen in Fig. 2 that the resultant ADF heights (in green solid curves) are very close to the quantum counterpart (in red broken curves). However, at some places the $|X(t)|$ is still too high, although the singularities have been all suppressed. This behavior suggests that $|\eta_J(t)|$ in the direction of $\Delta\mathbf{Q}^J(t) \to 0$ is not large enough.

The quantum ADF has thus dramatically improved the semiclassical ADF, and they are already good enough in the practical applications. Nonetheless, we keep exploring the geometry of the semiclassical singularity to take more proper account of quantum nature.

2. Collapse of the deviation-vector manifolds

In view of the above finding that the resultant $X(t)$ depends considerably on the choice of initial deviation vectors, we need to survey the geometry of manifolds composed of those

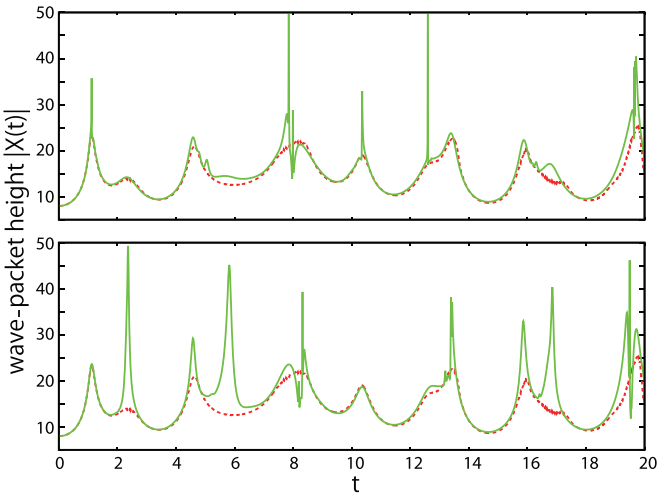

FIG. 2. (Color) Comparison between the FQ (red curve) and ADF (green curve) wave-packet heights is shown for two different spatial orientations of the initial deviation vectors but having the same $\sigma(0)$. It is confirmed that the time evolution of the wave-packet height on the reference classical trajectory is considerably dependent on the initial orientation.

deviation vectors by increasing the number of the initial sets of them. As in the above section, we calculate the ADF height in the same system as follows: (i) At $t = 0$, several nearby trajectories more than two sets are prepared with different orientations with respect to the original (xy) coordinate system, but all having a common value of $\sigma(0)$. (ii) All the nearby and the reference trajectories are launched with the common initial momentum to represent a same coherent-type Gaussian wave packet. (iii) At each time step, the lowest height out of the resultant set of $X(t)'s$ is adopted as ADF. The ADF height thus obtained is compared with the FQ counterpart in Fig. 3. In this figure, we applied this "variational" approach

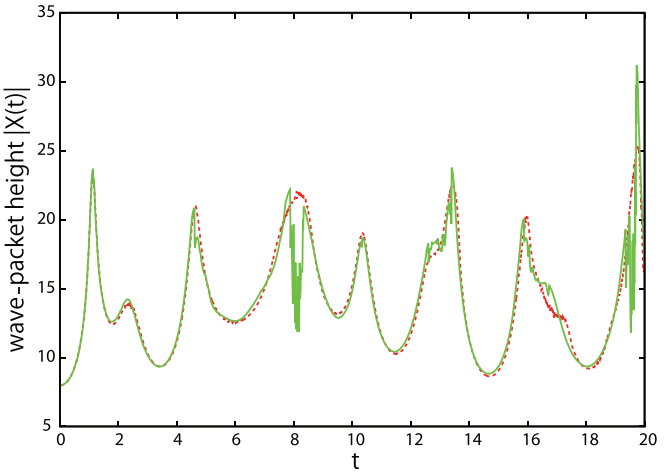

FIG. 3. (Color) The lowest ADF height obtained from seven initial orientations of the deviation vectors is plotted at each time step (in green curve). Red curve represents the corresponding FQ height. The variational approach has dramatically improved the description of wave packet except for the behavior near $t = 8$ and 19.5, when near degeneracy in $\sigma(t) = 0$ is observed.

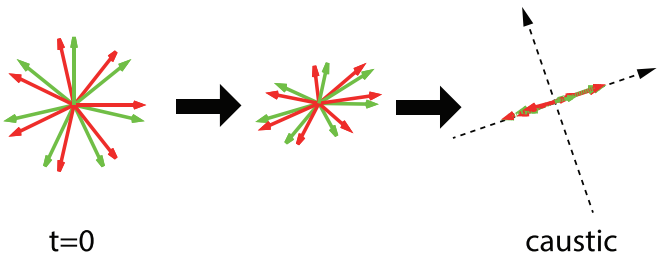

FIG. 4. (Color) (Leftmost) Seven deviation vectors to be denoted as $\Delta\mathbf{Q}^1(0)$ (red arrows) and those as $\Delta\mathbf{Q}^2(0)$ (green arrows) are prepared at $t = 0$ to form tiny squares on the reference trajectory. (Middle and rightmost) Time evolution of all nearby and the reference trajectories leads to collapse of the manifold, whose direction is found to be the same irrespective of the initial choice of deviation vectors.

with seven initial sets of the deviation vectors. It is found that description of the wave-packet height is dramatically improved by this procedure (compare each panel of Fig. 2 with Fig. 3).

The above variational approach is not necessarily practical, in particular, in systems of higher dimensions. However, the method should certainly reflect a variational nature behind the geometry of nearby orbits. To identify it, let us track the history of seven sets of deviation vectors $[\Delta\mathbf{Q}^1(t), \Delta\mathbf{Q}^2(t)]$, which were used in the calculation of Fig. 3. In Fig. 4, selected snapshots of the evolving deviation vectors are picked up along the reference path. They are as follows: at $t = 0$ (left), at a time hitting a caustic (right), and at some time in-between (center). It is seen that the manifold expanded by the initial deviation vectors begins to become elliptic and collapses (flattens) at a singular point. It is in the direction of zero diameter of this manifold that semiclassical singularity takes place and an appropriate value of $\eta(t)$ is essentially required. Incidentally, note that the collapse of the surrounding manifold of a reference path is a property of each reference path. Hence, the orientation of collapsing vector and its orthogonal complementary subspace do not depend on the choice of the initial deviation vectors, provided that nearby orbits lie close enough to the reference path.

To estimate the appropriate value of $\eta(t)$, we at least need to know the true direction that makes $\sigma(t)$ zero. In addition, the correct value of $\dot{\sigma}(t)$ [when $\sigma(t) = 0$] in this true direction is necessary as is indicated in Eq. (57). On the other hand, any deviation vector that passes across the collapsed manifold can bear zero length, even if it does not lie on the true collapsing vector. For such a vector, its direction deviates from the true one and makes a skew angle (smaller than the right angle) with the collapsed manifold (collapsing hyperplane). Therefore, those false vectors are expected to pass through the collapsing manifold with a higher speed than the true one, and it is anticipated that $|\dot{\sigma}(t)|$ at time $\sigma(t) = 0$ should be larger than that of the true deviation vector. Hence, due to the relation of Eq. (57), $|\eta(t)|$ tends to be estimated smaller than the correct one. Indeed, in the above example with use of the seven sets of deviation vectors, one of the deviation vectors has zero length and lies in the direction perpendicular to the survived manifold (see the rightmost figure in Fig. 4), thus making $|\eta(t)|$ at caustics largest.

3. *Search for the true collapsing direction in terms of the largest length of momentum gradient vector*

We next attempt to devise a systematic method to detect the true collapsing direction of the manifold of nearby orbits using only a small number of sets, hopefully one set, of nearby trajectories. To be more precise, we try to find a way to detect the direction in which the Wronskian relation may be correctly applied. We assume that the collapsing direction is one dimensional, that is, the zero of the deviation determinant $\sigma(t)$ is not degenerate.

First, we note that at a caustic point the magnitude of the momentum gradient in the true deviation direction, say, $\Delta\mathbf{e}^{\rm true}(t)$, is divergent. As shown in Eq. (53) of paper I [1], $\dot{\sigma}_{\rm true}(t)/\sigma_{\rm true}(t)$ is equivalent to the momentum gradient at t in the direction $\Delta\mathbf{e}^{\rm true}(t)$. Therefore, it is anticipated that if one keeps tracking the direction in which $|\dot{\sigma}_J(t)/\sigma_J(t)|$ takes the largest value, it should smoothly coincide with the true collapsing direction. Hence, we attempt to use a condition

$$\left|\frac{\dot{\sigma}_J(t)}{\sigma_J(t)}\right| \text{ to be maximized} \tag{83}$$

in order to find the appropriate $\Delta\mathbf{Q}^{\rm true}(t)$ and its associated momentum $\Delta\mathbf{P}^{\rm true}(t)$. Note that $\Delta\mathbf{P}^{\rm true}(t)$ is parallel to this collapsing direction.

Following the above guiding principle, we devise a method to apply this variational principle to a two-dimensional system. An extension to many-dimensional systems will be discussed later. Suppose we have a set of two nearby orbits $[\mathbf{q}^1(t), \mathbf{p}^1(t)]$ and $[\mathbf{q}^2(t), \mathbf{p}^2(t)]$ for a reference path $[\mathbf{q}^0(t), \mathbf{p}^0(t)]$. To find a direction that satisfies the above condition, we linearly transform the deviation vectors with an angle parameter φ:

$$\Delta\mathbf{Q}^1(t) = (\cos\varphi)\Delta\mathbf{q}^1(t) + (-\sin\varphi)\Delta\mathbf{q}^2(t), \tag{84}$$

$$\Delta\mathbf{Q}^2(t) = (\sin\varphi)\Delta\mathbf{q}^1(t) + (\cos\varphi)\Delta\mathbf{q}^2(t), \tag{85}$$

where $\Delta\mathbf{q}^J(t) = \mathbf{q}^J(t) - \mathbf{q}^0(t)$. $\Delta\mathbf{Q}^1(t)$ and $\Delta\mathbf{Q}^2(t)$ are required to be mutually orthogonal although the original $\Delta\mathbf{q}^J(t)$ are not necessarily orthogonal to each other. In this coordinate transformation, we choose an orthogonal matrix since we want to conserve the value of $\sigma(t)$. Deviation vectors and forces for the corresponding momentum are also transformed with the same transformation matrix, leading to $\Delta\mathbf{P}^J(t)$ and $\Delta\mathbf{F}^J(t)$. As before, $\dot{\sigma}_J(t)$ and $\ddot{\sigma}_J(t)$ are obtained by projecting those vectors onto the corresponding $\Delta\mathbf{Q}^J(t)$, respectively. Explicit expressions for the optimized value of φ are given in Appendix B.

We numerically apply this variational principle to the system represented in Eq. (80). Only one set of nearby orbits is randomly selected and tracked. In Fig. 5, the resultant ADF height is compared with the FQ counterpart. It is seen that agreement is excellent. (Note a possibility that the full quantum calculation using the grid FFT method may miss the true kinks that should appear in Fig. 5.) We have also confirmed that $\Delta\mathbf{P}(t)$ associated with $\Delta\mathbf{Q}(t) = 0$ is indeed parallel to the the collapsing direction [more precisely, parallel to $\Delta\mathbf{Q}(t^* + \varepsilon)$ with an infinitesimal ε for $\Delta\mathbf{Q}(t^*) = 0$], which supports numerically that the true collapsing direction has been well detected by this variational method. Comparing with the corresponding semiclassical ADF in the lower panel of Fig. 5,

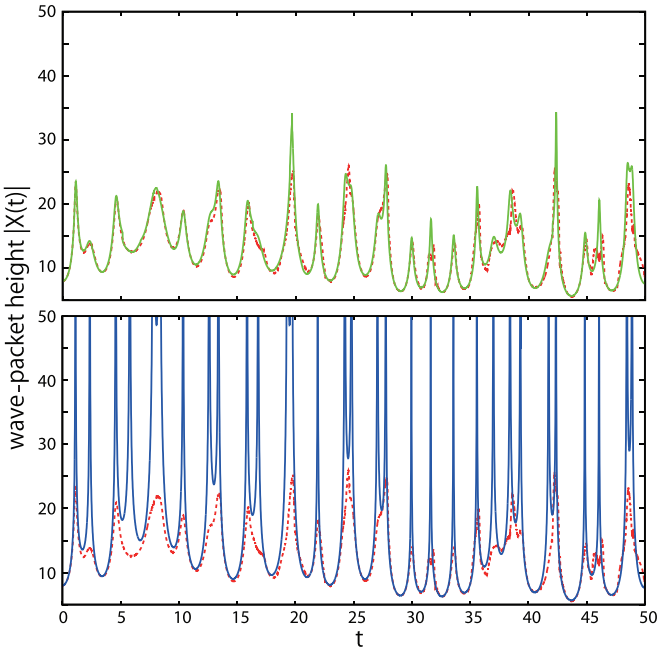

FIG. 5. (Color) (Upper panel) ADF height obtained with use of the maximization condition of $|\dot{\sigma}/\sigma|$ (green solid curve) is compared with the FQ counterpart (red dashed curve) for the system of Figs. 2 and 3 with an extension to a longer time. In the lower panel, the semiclassical ADF height is reproduced for comparison (blue solid curve), in which many divergent points are seen.

we immediately realize that the present quantum ADF is in a different stage from that of the semiclassical version.

4. Application to many-dimensional systems

Finally, we attempt to apply the above procedure to multidimensional systems. Here again, we start with $\sigma(t)$, which is invariant with respect to a coordinate transformation. Let us take an arbitrarily chosen plane expanded by two deviation vectors $\Delta\mathbf{q}^I(t)$ and $\Delta\mathbf{q}^K(t)$. Transformation in N-dimensional systems is performed with the product of two-by-two rotation matrices including a rotation angle in a plane made of two vectors

$$\begin{pmatrix} \ddots & & & & \\ & \cos\varphi_{IK} & \dots & -\sin\varphi_{IK} & \\ & & \ddots & & \\ & \sin\varphi_{IK} & \dots & \cos\varphi_{IK} & \\ & & & & \ddots \end{pmatrix}. \tag{86}$$

For $\Delta\mathbf{q}^I(t)$ and $\Delta\mathbf{q}^K(t)$, parameter φ_{IK} is calculated in the same way as performed in the two-dimensional case. This leads to the optimal direction within that particular plane. This two-by-two procedure is repeated until the convergence is attained, finally leading to $\sigma_J(t)$ in the collapse direction. After finding such a collapsing direction, we simply orthogonalize all the remaining deviation vectors $\Delta\mathbf{q}^I(t)$ using the Gram-Schmidt method. Next, we solve the Wronskian relation in each direction (coordinate) to attain $\sigma_J(t) + i\eta_J(t)$. Even the simple orthogonalization procedure should work accurately as suggested in Fig. 2, unless $\sigma_J(t)$ in a direction J thus determined happens to be very small.

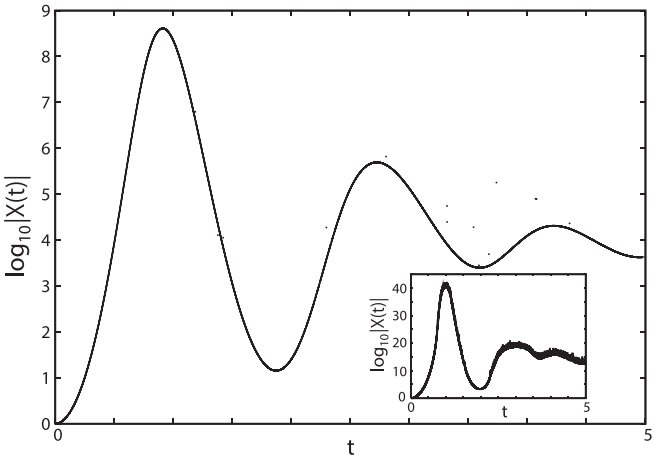

FIG. 6. Height of the quantum ADF obtained for a 100-dimensional test system. The height is dramatically lowered by the quantum diffusion. Note that in this test the initial wave-packet height is set to unity. In the inset, the corresponding semiclassical result is shown (note the scale).

A numerical example is shown in Fig. 6. In this test, a time evolution of the ADF height in a 100-dimensional system, whose Hamiltonian is

$$H = \sum_j^N \frac{p_j^2}{2m} + \sum_j^N \frac{\omega_j}{2}(q_j - R_{0j})^2 - \sum_j^{N-1} D_j(q_{j+1} - q_j)\exp[-\zeta_j(q_{j+1} - q_j)], \tag{87}$$

is tracked, where $N = 100$, $m = 1$, $R_{0j} = 2.0 \times j$, and $\omega_j = \omega_0 \times (1.013)^j$ with $\omega_0 = 1.0$ ($\omega_{100} \simeq 3.6387$). The Planck constant is set to $\hbar = 1.0$. This Hamiltonian models an energy-transfer dynamics in linearly chained oscillators. Couplings are considered only between the neighboring oscillators. $D_j = 1.0$ and $\zeta_j = 0.2$ are set to be the same for all the couplings. $X(0)$ was set to unity in choosing the initial conditions. The time step in the present ADF calculations is $\Delta t = 10^{-3}$. As we have observed in paper I, $|X(t)|$ rises very rapidly since all the oscillators come to their caustics near the time $t = 1$. As shown in the inset of Fig. 6, the height of semiclassical ADF (neglecting the quantum diffusion) is lifted up to the order of 10^{45}. On the other hand, the quantum ADF is suppressed below the order of 10^9 (see the main panel of Fig. 6). As noted in paper I, the semiclassical ADF suffers from very many divergences, although only the spikes of finite height are seen, which are in fact associated with divergence. This is because our chosen time interval (actually $\Delta t = 10^{-5}$ in semiclassical calculations in paper I) to calculate $\sigma(t)$ did not coincide with the exact timings of $\sigma(t) = 0$. Nevertheless, it is extremely interesting that the global features of both ADFs are seemingly similar to each other in the visual image of the graphs, although the absolute values are different in the order of 10^{35}.

In the graph for the quantum ADF, we notice that some small number of points do not lie on the smooth curve. This

is mainly due to insufficient convergence in the above two-by-two search for the maximum value of $\dot{\sigma}_J(t)/\sigma_J(t)$. More precisely, the insufficient convergence is often encountered when the deviation matrix has degenerate roots that give $\sigma(t) = 0$, that is, when there are more than one collapsing direction simultaneously. Such degeneracy is readily detected by examining the behavior of $\sigma(t)$ around the timings of $\sigma(t) = 0$. Obviously, we need another strategy to cope with this situation. Technically, however, such a difficulty can be avoided with use of the interpolation technique since the global feature of $X(t)$ is clear and the degeneracy is rather a rare event.

We have thus shown that the quantum ADF can be applied to systems of large dimensions without divergence.

V. CONCLUDING REMARKS

A theory of many-dimensional real-time quantum dynamics has been studied in terms of the action decomposed function (ADF) in this and the preceding companion papers. Following paper I, in which the time evolution of a wave function is described in terms of the deviation determinant and its resulting phases, this paper has been devoted to a study of the mechanism of quantum diffusion (quantum smoothing) that removes the semiclassical singularity. The deviation determinant reflects phase-space dynamics nearby a reference path, along which an ADF is supposed to be carried. We have proposed a Lorentzian form of the amplitude factor of ADF, the real part of which comes from the deviation determinant, while the imaginary part is proportional to the magnitude of the Planck constant, thus playing the role of smoothing the semiclassical singularity in ADF.

It has been found that the length of a deviation vector and the imaginary part of the Lorentzian mutually couple in a Wronskian relation. A number of theoretical advantages of the Wronskian relation have been illustrated in actual numerical calculations. Among others, it should be stressed that there is no essential difficulty in practical applications to many-dimensional heavy-particle systems like those in chemical reactions.

Finally, we have discussed a quantum mechanical time propagation of ADF in such a way that the value of it is carried from a point to another with quantum mechanical modulation arising from momentum gradient and quantum diffusion. Those ideas have been verified by comparing the ADF with the corresponding full quantum wave functions at each space-time point along classical trajectories. This is the most stringent test one can impose on this kind of study. However, what we need in our actual applications are quite often integrated quantities such as the S matrix and transition probabilities. The construction of ADF thus far presented in this paper is not so designed, and pointwise propagation may not be always useful in actual applications. Extension of the method in this aspect is under way and will be reported shortly.

ACKNOWLEDGMENT

This work was supported in part by a Grant-in-Aid for Scientific Research from the Ministry of Education and Science in Japan.

APPENDIX A: SOLVING THE WRONSKIAN

One of the theoretical advantages of the Wronskian relation is that it can be solved with a local approximation at a given time t, provided that $\sigma(t)$, $\dot{\sigma}(t)$, and $\ddot{\sigma}(t)$ are given. This is in a contrast to the calculations of stability matrix, which need a continuous integration of the relevant $(2N \times 2N)$-dimensional ordinary differential equations. First, let us assume that we have $\sigma(t)$ at three mutually close time points t_{-1}, t_0, t_1 as $\{\sigma(t_{-1}), \sigma(t_0), \sigma(t_1)\}$. These three points are used to fit with a sine function

$$\sigma(t) = A_\sigma \sin[\alpha(t - t_0) + \beta] \tag{A1}$$

only in the close vicinity of $t = t_0$. Then, we have $\sigma(t_0) = A_\sigma \sin\beta$, $\dot{\sigma}(t_0) = A_\sigma\alpha\cos\beta$, and $\ddot{\sigma}(t_0) = -A_\sigma\alpha^2\sin\beta$. The Wronskian relation specifies $\varsigma(t)$ in the form

$$\varsigma(t) \simeq B_\sigma \cos[\alpha(t - t_0) + \beta], \tag{A2}$$

where B_σ is to be determined in the Wronskian relation such that

$$\sigma(t)\dot{\varsigma}(t) - \dot{\sigma}(t)\varsigma(t) = -A_\sigma B_\sigma\alpha = a \tag{A3}$$

and therefore

$$B_\sigma = -\frac{a}{A_\sigma\alpha}. \tag{A4}$$

Note that only the product $A_\sigma\alpha$ is required, but not the individual terms A_σ and α. Thus, we have

$$\eta(t_0) = B_0\varsigma(t_0) = -B_0\frac{a}{A_\sigma\alpha}\cos(\beta). \tag{A5}$$

Obviously, the above treatments with sine and cosine functions are valid only when $\sigma(t_0)\ddot{\sigma}(t_0) < 0$. In the case of $\sigma(t_0)\ddot{\sigma}(t_0) > 0$, one can adopt hyperbolic-sine and hyperbolic-cosine functions instead, and the similar procedure may be applied.

In the approximation using the trigonometric functions, it is readily seen that the singularity is clearly avoided as follows. At the singular point, let $t_0 = t^*$, and

$$\sigma(t^*) \simeq A_\sigma \sin(\beta) = 0, \tag{A6}$$

resulting in $\beta = 0$. Then,

$$\dot{\sigma}(t^*) = A_\sigma\alpha\cos\beta = A_\sigma\alpha \tag{A7}$$

and therefore Eq. (A4) gives

$$B_\sigma = -\frac{a}{A_\sigma\alpha} = -\frac{a}{\dot{\sigma}(t^*)}, \tag{A8}$$

and Eq. (A2) leads to

$$\varsigma(t^*) = -B_\sigma = -\frac{a}{\dot{\sigma}(t^*),} \tag{A9}$$

which is equivalent to Eq. (57). This suggests a validity of using the local approximation.

APPENDIX B: SOLUTION OF THE VARIATIONAL PRINCIPLE WITH $|\dot{\sigma}_J(t)/\sigma_J(t)|$

The condition of Eq. (83) is formulated as

$$\frac{d}{d\varphi}\left(\frac{\dot{\sigma}_J(t)}{\sigma_J(t)}\right) = \frac{|\Delta\mathbf{Q}^J(t)|^2 \frac{d}{d\varphi}[\Delta\mathbf{Q}^J(t)\cdot\Delta\mathbf{P}^J(t)] - [\Delta\mathbf{Q}^J(t)\cdot\Delta\mathbf{P}^J(t)]\frac{d}{d\varphi}|\Delta\mathbf{Q}^J(t)|^2}{|\Delta\mathbf{Q}^J(t)|^4} = 0 \tag{B1}$$

with the solution being found as

$$\varphi = -\arctan\left(\frac{a_1b_3 - a_3b_1 \pm \sqrt{a_1^2b_3^2 - 2a_1b_3a_3b_1 + a_3^2b_1^2 - a_1b_2a_2b_3 + a_2^2b_1b_3 + a_1b_2^2a_3 - a_2b_1a_3b_2}}{(a_2b_3 - a_3b_2)}\right), \tag{B2}$$

where the following quantities are used:

$$\begin{aligned} &a_1 = \Delta\mathbf{q}^1\cdot\Delta\mathbf{p}^1, \quad a_2 = -(\Delta\mathbf{q}^1\cdot\Delta\mathbf{p}^2 + \Delta\mathbf{q}^2\cdot\Delta\mathbf{p}^1), \quad a_3 = \Delta\mathbf{q}^2\cdot\Delta\mathbf{p}^2, \\ &b_1 = |\Delta\mathbf{q}^1|^2, \quad b_2 = -2\Delta\mathbf{q}^1\cdot\Delta\mathbf{q}^2, \quad b_3 = |\Delta\mathbf{q}^2|^2. \end{aligned} \tag{B3}$$

The $\pm$ sign in the square root should be appropriately chosen to pick the maximum value.

[1] S. Takahashi and K. Takatsuka, preceding paper, Phys. Rev. A **89**, 012108 (2014).
[2] K. Takatsuka and A. Inoue, Phys. Rev. Lett. **78**, 1404 (1997); A. Inoue-Ushiyama and K. Takatsuka, Phys. Rev. A **59**, 3256 (1999).
[3] R. E. Wyatt, *Quantum Dynamics with Trajectories* (Springer, New York, 2005).
[4] C. L. Lopreore and R. E. Wyatt, Phys. Rev. Lett. **82**, 5190 (1999).
[5] D. Babyuk and R. E. Wyatt, J. Chem. Phys. **124**, 214109 (2006); **125**, 064112 (2006).
[6] L. S. Schulman, *Techniques and Applications of Path Integration* (Wiley, New York, 1981).
[7] J. H. van Vleck, Proc. Natl. Acad. Sci. USA **14**, 176 (1928).
[8] M. C. Gutzwiller, J. Math. Phys. **8**, 1979 (1967).
[9] W. H. Miller, Adv. Chem. Phys. **25**, 69 (1974).
[10] K. Takatsuka, S. Takahashi, K. Y. W. Patrick, and T. Yamashita, J. Chem. Phys. **126**, 021104 (2007).
[11] S. Takahashi and K. Takatsuka, J. Chem. Phys. **127**, 084112 (2007).
[12] J. Y. Fang and C. C. Martens, J. Chem. Phys. **105**, 9072 (1996).
[13] H. Wang, M. Thoss, K. L. Sorge, R. Gelabert, X. Giménez, and W. H. Miller, J. Chem. Phys. **114**, 2562 (2001).
[14] K. Takahashi and K. Ikeda, J. Chem. Phys. **99**, 8680 (1993).